IEEE Access
Multidisciplinary | Rapid Review | Open Access Journal

Received October 26, 2021, accepted December 6, 2021, date of publication December 10, 2021,
date of current version December 27, 2021.

*Digital Object Identifier 10.1109/ACCESS.2021.3134262*

# Wearable Accelerometer Layout Optimization for Activity Recognition Based on Swarm Intelligence and User Preference

**CHENGSHUO XIA AND YUTA SUGIURA**
Graduate School of Science and Technology, Keio University, Yokohama 223-8522, Japan

Corresponding author: Chengshuo Xia (csxia@keio.jp)

This work was supported by the Japan Science and Technology Agency (JST) Precursory Research for Embryonic Science and Technology (PRESTO) Program under Grant JPMJPR17J4.

**ABSTRACT** Wearable intelligent systems that recognize the daily activities of humans have significantly contributed to many useful applications. However, in practical wearable applications, the target individuals may have different body conditions and demands in terms of sensor wearing. Sensors may return different information depending on their placement, which to some extent determines the quality of a recognition system. Obtaining the optimal sensor positions with the highest recognition accuracy plays a significant role in activity recognition design. To contribute to a flexible and user-friendly wearable sensor layout, this paper designed a multistage and multiswarm discrete particle swarm optimization algorithm to explore the best sensor combinations and accuracy trends corresponding to different requirements of sensor numbers. The proposed optimization scheme is applied to investigate the influences that different numbers and placements of wearable accelerometers have on an activity recognition system. Furthermore, to address the issue of user preference regarding the sensor position, a relevant sensor layout can also be designed based on the demands and physical condition of the subject. The proposed method can determine the best sensor position (combinations) with lower computational cost for various activity recognition systems.

**INDEX TERMS** Motion recognition, optimal sensor placement, particle swarm optimization, wearable accelerometer.

## I. INTRODUCTION

The recognition of human activity has drawn much attention from multiple disciplines and applied scenarios. The systems used in this endeavor have enhanced people's lives due to their convenience and high performance in domains such as health rehabilitation [4], injury prevention [5], and diagnosis [6], among others. Human activity recognition (HAR), as the core technique to identify the human's motion type, is becoming a significant target of investigation [7]–[9]. The activities of daily living, motions of rehabilitation exercises, and other specific activities can all be designated as the recognized goals to aid specific types of people in their daily lives.

Based on the attributes and techniques of the devices these systems employ, HAR systems can be simply divided into nonwearable and wearable types. The former normally uses a camera and a deep learning network based on video streaming to recognize the human body [10]. Privacy concerns and the space limitations for locating the user are bottlenecks of this technique, although it does generate remarkable recognition results. To enable the subject to move in a wider range, based on the inertial measurement unit (IMU), many studies have been conducted to develop wearable HAR systems [11]–[13]. Both the handcrafted feature-based classifier and the deep network exist to facilitate the development of a corresponding system [14]–[16].

Since accelerometers can acquire information about the physical features of human motion, investigations have concentrated on adopting wearable accelerometers for human motion or gesture recognition [17]–[19]. Currently, increasing attention in the HAR field has been focused on off-the-shelf commercial electronic products embedded with accelerometers, such as smartwatches, smartphones, etc.

The associate editor coordinating the review of this manuscript and approving it for publication was Aasia Khanum.

However, these types of systems only provide a limited interface for users and require the devices to be attached to designated locations on the body, such as the wrist or the trouser pocket. In practical, the human body can be abstracted into a multi-segment rigid body model, and various segments of the body can present alterations of acceleration during activities. So, when combined with clothing and accessories, wearable sensors can be placed on the body in various positions from the head to the foot. Prior studies related to the sensor positions normally concentrated on the position specific HAR system or the transfer learning cross the different sensor position [20], [21]. Nevertheless, the examined sensor positions still maintain the less number and fails to generate the optimal sensor positions under the different conditions.

From the perspective of human-computer interaction, HAR combined with consumer electronics enhances convenience and availability, while sensor placement considering the practical requirements and physical condition of the user is still necessary. For example, in some cases, the monitored subject may be a patient with a specific disease or physical condition such as lacking one or more limbs and thus unable to wear the sensor on the established location [22]. For long-term monitoring, a fixed location can also cause discomfort to users. Considering the foregoing, a specific position on the human body is not conducive for all subjects due to the differences in demand. Moreover, a wearable system with specific sensor types can only generate limited data and provide scant robustness against placements on different parts of the body. Even if a state-of-the-art deep network is employed, the effect caused by the different positions of the sensors cannot be eliminated [23]. Therefore, seeking a favorable sensor position to improve the relevant recognition accuracy as well as balance the recognition results and the user's conditions can be an effective compromise scheme. This paper intends to evaluate all the possible obvious sensor placements on the body and design an optimization scheme to generate sensor layout with respect to best accuracy under different scenarios. The main contributions of this work can be summarized as follows:

1. A swarm intelligence-based algorithm has been developed for solving such sensor combinational optimization problems with lower computational times.

2. The potential locations of wearable accelerometers on the human body have all been examined using different combinations and numbers of sensors to explore the best sensor layout and the accuracy trend against different types of activities.

3. A series of results based on specific positions of user preference on the human body with different adopted sensor numbers are presented.

## II. RELATED WORK

HAR systems are categorized according to the equipment used and the various approaches, including the classifier establishment, data processing, and fusion method [24]. Wearable systems have emerged from calculations of the obvious variations of signals reflecting human motion. For this type of system, the accelerometer has been widely utilized for activity recognition and subsequent applications. The accelerometer can be not only embedded in consumer electronics to increase convenience but also specialized to monitor specific people's activity and conduct related applications [25], [26]. Most studies have been dedicated to improving the existing classifier structure to fit more ubiquitous devices and form a pervasive sensing system [27]–[29]. However, the single sensor used sometimes is not adequately accurate. If more than one sensor is used, the selection of the sensors' positions needs to be considered. Optimal sensor placement is an issue that has received extensive attention in several domains. Given the limitations of the sensed subjects, multiple quantities or multimodal sensors are generally adopted to improve the performance of the perceiving system. To find the global best sensor sites or layout, the most effective method is trying every possible combination, but this carries high computational cost. Some heuristic optimization and greedy algorithms have been utilized to optimize the sensor layout. Blanloeuil *et al.* [30] adopted the particle swarm optimization method to optimize the ultrasonic structural health monitoring (SHM) system in a 2D coordinate. The results demonstrated that with the optimization, the performance of SHM can be enhanced to find more areas of defect. Flynn and Todd [31] established the fitness function with Bayesian approach between the sensor locations and the error criterion in the detection system and employed a genetic algorithm to optimize the sensor space. Mallardo *et al.* [32] abstracted the optimization task into a discrete issue. They defined the specific locations on the composite panels as the sensors' possible positions. An artificial neural network was adopted to build the object functions using the genetic algorithm to optimize the sensors' location. Swarm intelligence and an evolutionary algorithm have been designed to address the sensor space optimization issue effectively and improve performance.

However, for HAR systems based on wearable data, fewer schemes have been investigated with respect to optimal sensor placement. As the detected data from the wearable sensor contain physical characteristics of the motion to some extent, more sensor information will contribute to improved accuracy. In considering the characteristics of the system or the classifier, blindly increasing the number of sensors does not generate a good result. The inherent trade-off between the amount of sampled data and the recognition result emerges from this. Kunze and Lukowicz [33] presented an approach to compensate for the effects of the different sensor placements, namely, arranging the sensors in such a way as to give adequate performance, given that different parts of the human body contain different information regarding the activity being conducted. Atallah *et al.* [11] investigated optimal sensor placement for specific activities by means of the k-Nearest Neighbor (KNN) classifier. They also assessed the impact of selected features on classification results and

presented the best features related to each activity of daily living (ADL) group. Fourteen activities were examined and divided into five groups by intensity of activity. For these types of activity, different sensor positions generate different levels of accuracy. The study investigated the influence of a single sensor on daily activity recognition; however, the option of involving more sensors to improve the accuracy of the results was not discussed. Gjoreski and Gams [34] developed an ADL recognition system using one to three sensors on three different parts of the human body to recognize eight activities. However, only three potential locations are mentioned in their work, and only 69.8% accuracy was obtained via a random forest classifier when only a chest sensor was used. With two more sensors added, the average prediction accuracy increased to 94.3%. Olgum and Pentland [35] utilized the Hidden Markov Model (HMM) to classify eight common human daily activities. Again, three positions on the human body were considered. Using the SVM classifier, Cleland *et al.* [36] proposed a more complete work that employed six sensors placed on the human body, and all possible combinations of the six sensors were tested. They showed that the best single sensor location is on the hip, generating 96.66% accuracy. They also indicated that a two-sensor combination can provide reasonable results. When they evaluated all possible sensor combinations, all combinations achieved similar accuracy (differences were within 1%). Although these studies varied the number of sensors for measuring a specific activity, they demonstrate little comparison of different sensor placements.

Sztyler and Stuckenschmidt [20] added the process of predicting the on-body position of a wearable device before executing HAR. They conducted subject-specific and cross-subject validations, assuming the system could be used with the labelled data and under the condition that the user could not produce the training data. After comparing seven different body parts, they recognized the waist as the most suitable position. Additionally, Kurban and Yildirim [37] investigated several classifiers with three common positions on the human body. They used the HAR system to classify five simple activities, and the chest was identified as the best sensor placement.

Thus, various researchers have utilized different machine learning models for HAR to study the influence of sensor placement on accuracy. However, as stated in [20], the optimal sensor placement depends on the recognized activities. The factors affecting the system accuracy are complicated, including the sensor position, the selected learning network, and the method for processing the sampled data. It is meaningless to evaluate the optimal sensor layout without the specific HAR system and the recognized activities as the premise. Based on these previous studies, this paper proposes an optimization scheme to offer the best wearable sensor layout to fit the user's requirements. The designed scheme is effective once the adopted HAR system and dataset are determined. In contrast to other works, we expanded the potential sensor placement over the whole body according to the human motion rigid-body model, and 17 different parts of the human body were examined. Based on our HAR system and dataset, the proposed optimization approach can generate the optimal sensor layout for different numbers of sensors as well as make recommendations for sensor placement under particular sensor requirements.

## III. WEARABLE ACCELEROMETER LAYOUT OPTIMIZATION SCHEME

### A. GREEDY APPROACH (COMBINATIONAL METHOD)

To investigate the optimal combination of sensors under different requirements of sensor numbers, we first considered the greedy approach due to its lower computational times. The greedy method merely generates the optimal solution based on the current best solution. It requires first determining the best position for a single sensor, $S_{\mathrm{op1}}$. To this end, the acceleration data from 17 sensors were used to train and test the model, and thus, the optimal sensor use could be identified. We subsequently combined $S_{\mathrm{op1}}$ with one of the remaining 16 sensors in turn and compared the results to find the best two-sensor combination, i.e., $S_{\mathrm{op1}} + S_{\mathrm{op2}}$. The adopted criterion is the maximum average accuracy of classification for 10 different activities. Each test was executed three times, and the average accuracy was calculated as the result. The solution was derived based on the previous best solution, and the result was normally the local optimal solution.

### B. MULTISTAGE AND MULTISWARM DISCRETE PARTICLE SWARM OPTIMIZATION (MSMS-DPSO)

The greedy method is likely to give a classification result related to different numbers and positions of sensors. This method trends toward accuracy, and the corresponding computational complexity is relatively low. However, the results obtained depend greatly on previous findings. Possible combinations other than those based on previous results are not tested (e.g., testing the combination of two positions with worse results). To avoid such issues, a heuristic global searching algorithm can be adopted.

A particle swarm optimization (PSO) algorithm as a type of heuristic algorithm imitates the behavior of birds foraging. The goal of the search is set as the best solution of the specific fitness function. The PSO algorithm normally generates a series of initial solutions within an $N$-dimensional space as a random distribution of particles. Each particle is assessed by the corresponding value of a specific fitness function, i.e., its fitness value. The particle has its own velocity of movement and position. With different forms of PSOs, each discrete PSO (DPSO) normally requires that the position of each particle should be an integer and not repeated in different dimensions [45]–[49]. Such discrete problem optimizations all follow the basic principle of updating the velocity of a particle and combining with other algorithms to update the position of the particle based on different problems.

For a DPSO algorithm, the velocity is updated by formula (1), where $i$ represents the current dimension.

The equation for updating velocity consists of three parts: a self part, an ''individual'' part, and a ''social'' part. The self part is based on the previous velocity and is normally multiplied by the weight $w$ to control the degree to which the previous velocity affects the current one. The ''individual'' part enables the particle to be close to the best position from its individual history, $P_{\text{best}}$. The $G_{\text{best}}$ is the core of the ''social'' part, which is the best position among the history of all particles. This part allows the particle to converge on the overall best position. The coefficients $r_1$ and $r_2$ are randomly produced from (0,1). $c_1$ and $c_2$ are operators of the ''individual'' part and the ''social'' part, respectively. The position is subsequently altered based on the new velocity of a particle, as shown in formula (2).

$$v_{n+1}^{i} = w \cdot v_{n}^{i} + c_1 r_1 (P_{best}^{i} - x_{n}^{\prime i}) + c_2 r_2 (G_{best}^{i} - x_{n}^{\prime i}) \quad (1)$$

$$x_{n+1}^{i} = x_{n}^{\prime i} + v_{n+1}^{i} \quad (2)$$

As a swarm intelligence algorithm, PSO emphasizes the randomness and convergence of the algorithm itself. The randomness requires the position of the particle concerned to be altered disorderly and freely. This is reflected in the principles of generating and updating velocity (random operators $r_1$ and $r_2$). For a convergence characteristic, it requires all the particles involved to be able to converge to the best position. Thereby, the ''social'' part of the velocity-updating formula provides the direction for the other particles. During the iteration period, all particles will ''fly'' to the global best position $G_{\text{best}}$, updating their positions based on fitness values. Thus, the characteristics of randomness and convergence constantly guarantee that particles may converge to find the best position. Relevant improvements from previous studies may concern ways to update particle position, like redefining the velocity operator, involving a sigmoid function, employing a hybrid searching algorithm, and so on. Hence, in this case, the final goal is to figure out the best optimal combinations among 17 sensor positions given the number of sensors required. It is vital to ensure the particles' movement and to avoid repetition in different dimensions. Thus, the methods of updating velocity and position used in this paper are not altered. We have designed a multistage and multiswarm discrete PSO (MSMS-DPSO) algorithm for optimal sensor combination searching. The dimensionality of space established is related to the quantity of sensors used on the human body. The relevant workflow of the MSMS-DPSO is shown in Figure. 1.

The main process of the algorithm can be divided into two periods: the first is intragroup optimization, and the second is whole swarm optimization. During the first period, different swarms carry out respective PSO optimization in their own swarms. The global best position and local best position are both defined within their group, and different swarms' best positions do not affect each other. In this period, the key point is to find the maximum fitness value by means of optimization within various swarms. The position corresponding to the maximum value among different swarms in each iteration needs to be recorded and updated as well. Once any dimension's position has been changed, the fitness value is calculated and used to update the local best position and the global best position. After the completion of intragroup optimization, the beginning of the second optimization period enables the selected particle to be the global best position from each swarm in first stage. The global best position at this moment is the optimal position among the global best positions of all swarms at the last step of the previous stage. In this period, both accelerating convergence and simultaneously testing other combinations are necessary, and the fitness calculation is performed after the positions of one particle in different dimensions have been all updated. The velocity limitation is also extended to quicken the particle's movement.

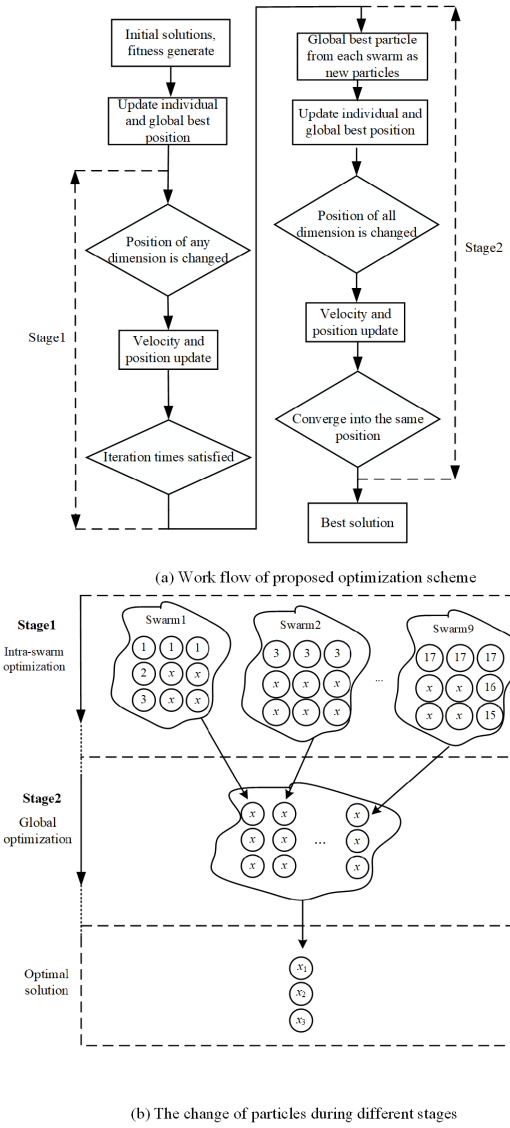


**FIGURE 1.** Operation of designed optimization method.

However, before applying the velocity- and position-updating formulas, the initial positions of all particles need to

be considered seriously. The initial positions of the particles could have a functional influence on the performance of a PSO [45]. In our paper, the position of the first dimension is assigned to the odd position. Two border particles ($[1, 2, 3 \ldots, N]$, $[17, 16, 15 \ldots, 17-N+1]$) are also defined to make sure the particle does not move out of bounds. These numbers indicate the position of the corresponding sensor. After the position of the first dimension has been specified, the position numbers of the remaining dimensions are chosen randomly and do not repeat the position of the first dimension.

The most important part of the optimization is the velocity and position updating process. Unlike a typical PSO algorithm, the velocity cannot simply be updated by formula. It needs to ensure that the particle position is not repeated in different dimensions and simultaneously ensure the ergodicity of the particle. After calculating velocity and position from equations (1) and (2), to obtain the discrete value, the calculated new position needs to be rounded using equation (3).

$$x'^{i}_{n+1} = \begin{cases} [x^{i}_{n+1}] & if\ x^{i}_{n+1} - [x^{i}_{n+1}] < 0.5 \\ [x^{i}_{n+1}] + 1 & if\ x^{i}_{n+1} - [x^{i}_{n+1}] > 0.5 \end{cases} \tag{3}$$

When $x'^{i}_{n+1}$ is equal to $x'^{i+1}_{n+1}$, a position repeat appears, and the algorithm requires processing to ensure that no dimension's position number is the same. When the new position $x'^{i}_{n+1}$ of dimension 1 has been calculated, it is subsequently checked against the positions of the other dimensions. If the current dimension's position $x'^{i}_{n+1}$ is equal to any of the positions of the remaining dimensions, its position number will decrease by 1, while convergence velocity $v < 0$ (as shown in Figure. 2.(a)). In addition, position limitation is necessary and needs to be accounted for during changes in position. The maximum position number is limited to 17, while the minimum value is 1. The corresponding implementation of MSMS-DPSO is shown in Algorithm 1 (see Appendix).

## IV. HUMAN ACTIVITY RECOGNITION SYSTEM DESIGN

### A. EXPERIMENTAL SETUP

#### 1) EXAMINED SENSOR POSITIONS

Considering the current positions of on-body consumer devices, potential wearing locations on the body, and the symmetry of the human body structure, devices were placed at 17 different positions via bandages on the body, including the head, chest, left shoulder, right shoulder, waist, left upper arm, left forearm, right upper arm, right forearm, left hand, right hand, left upper leg, left lower leg, left foot, right upper leg, right lower leg, and right foot. These positions include all possible active parts involved in daily activities and more or less cover all potential locations of sensors in current research [4]–[6]. We also listed the possible corresponding practical sensor installation locations combined with clothes, consumer electronics, and accessories according to 17 different body parts, as shown in Table 1. Details of the sensor locations on the human body are displayed in Figure 1.

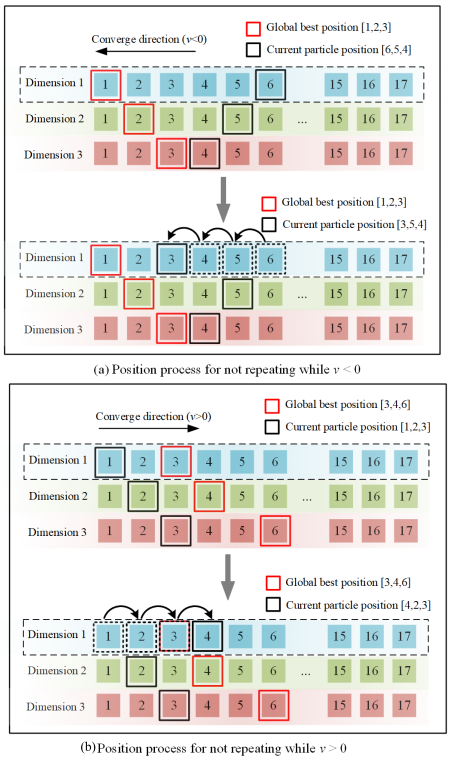


**FIGURE 2.** Position updating for not repeating (3-sensor example).

**TABLE 1.** Selected sensor positions and corresponding practical locations.

| Body part | Practical senor location |
|---|---|
| Head | Hair band/Glasses/Earphone |
| Chest | Shirt pocket/Necklace/Bra |
| Shoulder | Backpack straps |
| Upper arm | Armband |
| Forearm | Watch/Wristband |
| Waist | Belt |
| Upper leg | Trouser pocket |
| Lower leg | Knee supporter |
| Foot | Shoes |

#### 2) RECOGNIZED ACTIVITY

Ten different human daily activities were executed in the experiment to ensure a more comprehensive range of testing activities [12], [41], [42]. These activities can be divided into three groups: static activities, transitional activities, and dynamic activities (as shown in Table 2).

#### 3) DEVICE

Acceleration information was obtained from a wearable IMU device (Xsens MVN). The acceleration detected from a triaxial accelerometer in each unit was sampled at 60Hz.

#### 4) DATASET

As the tested sensor positions cross the whole body and there is no public dataset could satisfy the requirement of our

**TABLE 2.** Completed activities in the experiment.

| Type | Activity |
|---|---|
| Static | Standing, Lying |
| Dynamic | Walking, Running, Going upstairs, Going downstairs |
| Transitional | Sitting-to-standing, Standing-to-sitting, Squatting-to-standing, Standing-to-squatting |

experiment. We recorded the data for testing, which involved 10 subjects (5 males and 5 females) wearing 17 sensors on their bodies. The subjects' heights ranged from 160cm to 188cm, and the subjects were instructed to do the relevant activities naturally.

#### 5) PROCEDURE

The subjects were directed to perform static and dynamic activities for durations of 90 seconds at a time and transitional activities in sets of 15 repetitions. Data were recorded by the XSens MVN capture system, which can reconstruct a human model with visualization. This system can also perform annotation of related activities.

### B. DATA PROCESSING

Acceleration data from each axis was processed with segmentation via a sliding window method. According to Wang *et al.* [12], the length of the sliding window may directly affect the results of ADL prediction, regardless of the classifying methods chosen. Their study states that the window size should be larger than 2.5s to obtain acceptable accuracy. Therefore, the sliding window length in this work was set at 4s with an overlap of 2s to ensure continuity of motion.

### C. CLASSIFIER

Considering the characteristics of the dataset used, we adopted a classifier with handcrafted features. Li *et al.* [42] evaluated different classifiers with the same feature sets for HAR, and the best prediction result was shown by SVM compared with the KNN, FNN, and DT classifiers. SVM can map the data to high-dimensional space via a Kernel function to discover a hyperplane to classify the dataset [43]. Hence, SVM with the radial basis kernel function (RBF) is adopted in this paper to discriminate different human ADLs.

### D. FEATURE EXTRACTION

Normally, a sampled acceleration signal can be used to derive the orientation vector of acceleration [34]. Because the calculation of the orientation of acceleration is influenced by the sensor placement, the features used in this research are independent from the orientation vector but relate to statistical characteristics and the energy of the signal. Features involved in the human ADL recognition process are commonly divided into time-domain features, frequency-domain features, and time-frequency features [44]. Due to the significance of feature extraction, Atallah *et al.* [11] argued that the average entropy of the acceleration signal could have a relatively high ranking among 13 time-frequency features examined. Moreover, Preece *et al.* [44] also demonstrated that time-frequency features do not present an advantage compared with time-domain and frequency-domain features for the recognition of eight activities. Therefore, this work utilizes time-domain and frequency-domain features. The extracted features are listed in Table 3. All features shown are calculated from the signal of each axis.

**TABLE 3.** Extracted features and descriptions for classification.

| Type | Descriptions |
|---|---|
| Time domain | Mean, variance, standard variance, 75th percentile, inter-percentile |
| Frequency domain | Mean and median value of power spectrum, Shannon entropy |

## V. EVALUATION AND RESULTS

With the approach introduced above applied for seeking an optimal combination of sensors, this section will discuss the relevant results from the experiment.

The evaluation can be divided into three parts, at the first we evaluated the different sampling rate influence on the optimal sensor positions by the combinational method, which is able to figure out the basic trend of sensor number effect on classification accuracy. Secondly, our MSMS-DPSO method is evaluated. The baseline method is selected as the *Dynamic Programming*. The baseline method related to finding the global optimal position combinations, testing all the combinations of a given number of sensors. We would test how close the result from MSMS-DPSO to *Dynamic programming* and the computational times. Finally, we provide the usage of our method on deriving the optimal sensor positions according to the user preference.

### A. INFLUENCES OF DIFFERENT POSITIONS AND NUMBERS

#### 1) STUDY WITH GREEDY APPROACH (COMBINATIONAL METHOD) FOR DIFFERENT SAMPLING RATES

As introduced above, the greedy approach based on the best sensor position from the previous time can be used to generate the local optimal solution with less computational time. Furthermore, we also down-sampled the acceleration to validate a more practical situation and determined the impact of sampling rate on the best position. The dataset of 60Hz, 30Hz, and 20Hz sampling frequency was examined, and relevant results are shown in Table 4. Based on the results, with decreasing sampling frequency, the accuracy increased. However, the best positions and numbers of sensors were not significantly altered.

In this experiment, we used the 10-fold cross validation (CV) method to calculate the accuracy of mentioned sensor positions. The training data and testing data are separated

**TABLE 4.** The result of optimal combination method with different sampling frequency.

| No. | Sampling frequency | | | | | |
|---|---|---|---|---|---|---|
| | 60Hz | | 30Hz | | 20Hz | |
| | Position | Accuracy | Position | Accuracy | Position | Accuracy |
| 1 | Right shoulder | 88.61 | Right shoulder | 92.48 | Right shoulder | 94.09 |
| 2 | + Waist | 92.66 | + Waist | 95.55 | + Waist | 96.77 |
| 3 | + Chest | 94.14 | + Chest | 96.47 | + Chest | 97.31 |
| 4 | + Right upper arm | 94.59 | + Right upper arm | 97.34 | + Head | 98.09 |
| 5 | + Head | 95.33 | + Head | 97.81 | + Left forearm | 98.17 |
| 6 | + Left shoulder | 95.39 | + Left shoulder | 97.80 | + Right upper arm | 98.26 |
| 7 | + Left upper arm | 95.29 | + Left upper arm | 97.18 | + Right forearm | 97.97 |

**TABLE 5.** Parameter set for MSMS-DPSO during the testing.

| Parameter | | Value |
|---|---|---|
| Swarm size | | 9 |
| Particles in each swarm | | 3 |
| Dimensionality | | 2/3/4 |
| Inertial factor $w$ | | 0.6 |
| Velocity limitation $v_{\text{lim}}$ | | Intragroup period: ±1<br>Whole swarm period: ±1.6 |
| Individual factor $c_1$ | | Intragroup period: 2<br>Whole swarm period: 1 |
| Social factor $c_2$ | | 2 |
| $r_1$ | | Randomly taken from in [-1,1] |
| $r_2$ | | Randomly taken from in [-1,1] |
| Stop condition | Intragroup period | Maximum iteration times: $N$+1 |
| | Whole swarm period | Converge to one position |

independently and randomly with no overlapping for accuracy of calculation.

The results also show that the more sensors used for each sampling rate, the greater the total classification accuracy. Nevertheless, when five or more sensors are used, the increase in average classification accuracy is not obvious. This may be due to the overfitting of the SVM classifier. Also, in practical applications, it is more worthwhile for us to concentrate on investigating the use of four or fewer sensors. In this way, both actual application and the range of large changes in accuracy are taken into account.

### 2) STUDY WITH MSMS-DPSO APPROACH FOR DIFFERENT CLASSIFIERS

The MSMS-DPSO algorithm was only adopted to determine the best solution when using two, three, or four sensors. The parameters applied to the MSMS-DPSO algorithm in this paper are listed in Table 5.

In this experiment, the compared objects are from two points, the accuracy and computational times between our method and baseline method. For the accuracy calculation, to decrease the randomness of classification, the random environment was set as the same. and the examined dataset (including training and testing) was the same as well (the training and testing dataset are divided by 75% and 25% respectively). The computational times is the total number of accuracy calculations during the iteration.

HAR systems are diverse according to designed objects (i.e., recognized activities), adopted classifiers, data segmentation lengths, etc. It cannot be said which classification method has an absolute advantage among HAR systems. As the application of our algorithm is for a certain HAR system, it is necessary to validate the generalizability for different classification methods for the same recognized task. Therefore, we conducted an experiment that applied the MSMS-DPSO to several different classification approaches. Since we selected the SVM as the chief classifier for our study, the compared methods are (a) Random Forest (30 estimators), (b) baseline CNN classifier, (c) DNN+LSTM from [1], and (d) DeepCNN [3]. Methods (c) and (d) maintained the network structure described in the original papers. Method (b) is indicated as the baseline deep learning method, which consists of a 16-feature map with $2 \times 2$ kernels and Relu activation, a dropout layer with 0.1 rate, a 32-feature map with $2 \times 2$ kernels and Relu activation, a dropout layer with 0.2 rate, a flattened layer, a dense layer with 128 nodes and Relu activation, a dropout layer with 0.5 rate, and finally, a 10-node dense layer as output. The learning methods were developed based on TensorFlow 2.1 within Python 3.6 and GPU GTX 1080ti. The batch size and epoch were 30 and 20, respectively, for all learning methods. To decrease the randomness of classification, the random environment was set as the same, and the examined dataset (including training and validation) was the same as well. Additionally, the baseline method related to finding the global optimal position combinations, testing all the combinations of a given number of sensors, was executed to validate the results from the MSMS-DPSO. Figure 4 illustrates the working process of the MSMS-DPSO with three sensors as an example. The corresponding experimental results are presented in Table 6 and Figure 5.

As Figure 5 (a) to (e) shows, the effect from different classifiers is not significantly obvious for ADL recognition. This has been reported by other works as well [3], [15]. For example, in [3], the difference among the SVM and Random Forest classifiers and the deep learning network is less than 0.1%. This is mainly because the signal captured from the accelerometer maintains limited channels, and the recognized activities are relatively simple. Therefore, the deep learning-based classification method cannot extract more obvious features to outperform artificial feature-based classifiers, such as SVM and Random Forest. Because there were

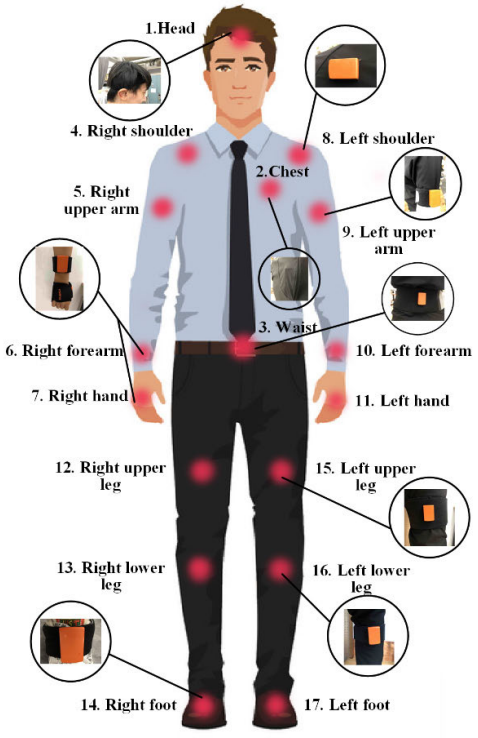


**FIGURE 3.** Locations for sensors worn on human body (with image of selected sensors). For generality, the Xsens sensors are attached to the commonly worn placement of the human body, such as the wrist, middle of thigh (as the pocket position), middle of forearm and so on.

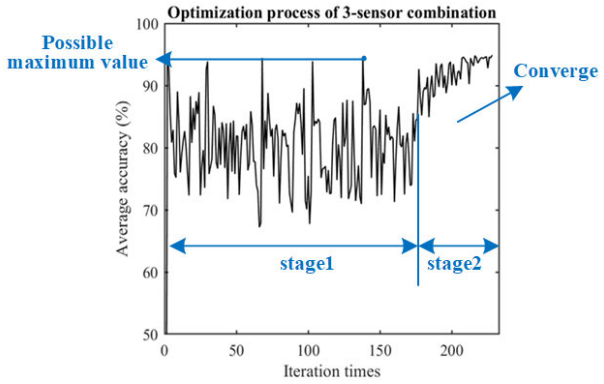


**FIGURE 4.** Convergence process of MSMS-DPSO (3-sensor of SVM classifier used as an example).

no significant differences among several classifiers except the baseline CNN, we still chose the SVM for subsequent analysis.

In terms of optimization, Table 6 and Figure 5 (f) demonstrate that the MSMS-DPSO can calculate the "best" sensor placement and combination. For lower sensor numbers, like two sensors used, MSMS-DPSO can more successfully find the global optimal positions compared with testing all combinations. With higher sensor numbers, the task is more challenging. In some cases, the result from the MSMS-DPSO was not the so-called global best position. This is because of the restricted particle searching feasibility of DPSO, which is prone to be trapped into the local optimum. Even so, the accuracy difference between the MSMS-DPSO and baseline

**TABLE 6.** Result of MSMS-DPSO method and comparison with all combinations tested for different types of classifiers with the same data. (M indicates the proposed MSMS-DPSO method, and A indicates the testing all combinations, i.e., baseline method).

| Classifier | Method | Sensor number | Position | Accuracy |
|---|---|---|---|---|
| SVM | M | 2 | Waist + Chest | 93.56% |
| | | 3 | Waist + Chest + Right Upper Arm | 94.57% |
| | | 4 | Waist + Chest + Head + Right Upper Arm | 95.13% |
| | A | 2 | Waist + Chest | 93.56% |
| | | 3 | Waist + Chest + Right Upper Arm | 94.57% |
| | | 4 | Waist + Chest + Head + Right Upper Arm | 95.13% |
| Random Forest | M | 2 | Right shoulder + Left foot | 94.10% |
| | | 3 | Right shoulder + Right hand + Left lower leg | 94.33% |
| | | 4 | Right Upper Arm + Left Shoulder +Left Hand + Right Foot | 94.78% |
| | A | 2 | Right shoulder + Left foot | 94.10% |
| | | 3 | Waist + Chest + Left Hand | 94.67% |
| | | 4 | Waist + Chest + Left Hand + Right Lower Leg | 94.89% |
| CNN | M | 2 | Left Shoulder + Left Foot | 91.49% |
| | | 3 | Chest + Right Shoulder + Left Foot | 91.97% |
| | | 4 | Right shoulder + Left shoulder +Left Upper Arm +Left Foot | 92.97% |
| | A | 2 | Left Shoulder + Left Foot | 91.49% |
| | | 3 | Chest + Right Shoulder + Left Foot | 91.97% |
| | | 4 | Waist + Chest +Right Lower Leg +Left Foot | 92.97% |
| DNNLSTM [1] | M | 2 | Right shoulder + Left foot | 92.97% |
| | | 3 | Right Upper Arm + Left Shoulder + Right Foot | 93.19% |
| | | 4 | Waist + Chest + Right Shoulder + Left Foot | 95.12% |
| | A | 2 | Right shoulder + Left foot | 92.97% |
| | | 3 | Chest + Right Shoulder + Right Foot | 94.67% |
| | | 4 | Waist + Chest + Right Shoulder + Left Foot | 95.12% |
| DeepCNN [3] | M | 2 | Right Shoulder + Left Foot | 92.40% |
| | | 3 | Head + Right Shoulder + Left Foot | 93.47% |
| | | 4 | Right Upper Arm + Left shoulder + Right Lower Leg + Left Foot | 95.23% |
| | A | 2 | Right Shoulder + Left Foot | 92.40% |
| | | 3 | Head + Right Shoulder + Left Foot | 93.47% |
| | | 4 | Waist + Chest + Head + Left Foot | 96.03% |

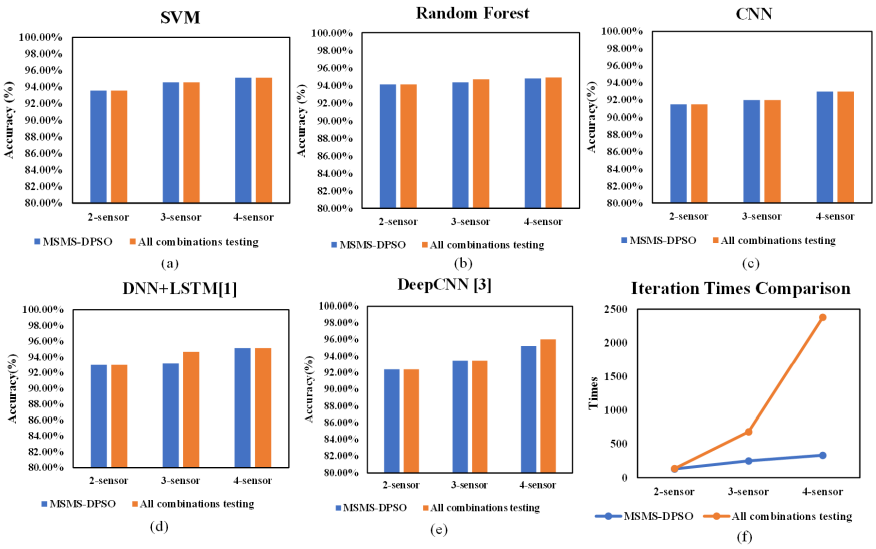


**FIGURE 5.** Test on different classification methods. (a) is SVM classifier; (b) is Random Forest classifier; (c) is CNN; (d) is from [1]; (e) is from [3]. (f) is computational cost comparison (average calculation from 5 tests with MSMS-DPSO). The proposed MSMS-DPSO method can utilize less computational time to be close to the baseline method and the accuracy results of two methods are closed.

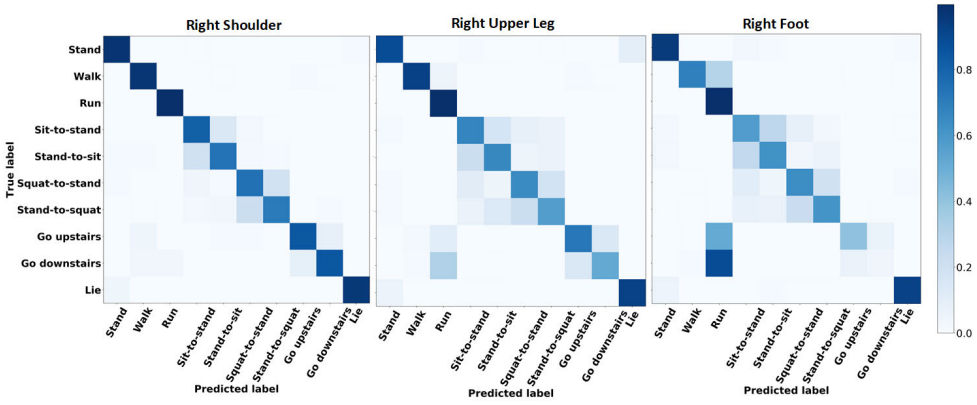


**FIGURE 6.** The confusion matrix of right shoulder sensor, right upper leg sensor, and right foot sensor.

methods is quite small (less than 1%). Because we stabilized the random characteristic of the selected learning method for algorithm comparison, different random characteristics would influence the results slightly, which may cause some differences between the results from the two methods. So, the designed MSMS-DPSO can be shown to effectively determine the optimal sensor position. Compared with the all-possible-combinations test, the computational time is lower, especially when the required number of sensors is higher.

### *B. DISCUSSION OF SENSOR LAYOUT*

#### 1) SINGLE SENSOR USED AMONG THE DIFFERENT BODY SEGMENTS

When using one accelerometer, the sensor placed on the right shoulder expresses a relatively higher average classification accuracy. Furthermore, sensors on the lower part of the human body normally result in worse accuracy, especially on the foot. The results from the sensors located behind the forearm (arms straight down naturally), except the waist sensor, are all relatively lower.

For the three types of activities involved, the classifier can provide different prediction results depending on the different positions of the sensors. Figure 6 displays the confusion matrix from the right shoulder, right upper leg, and right foot when using one sensor. The results show that the average prediction accuracy decreases as the sensor position moves down the body. Figure 7 presents the F1 scores of each single type of activity recognition corresponding to these three sensors.

Figures 6 and 7 together show that for static activity classification, there is no significant difference among the three sensor positions. The main factor that causes a decrease in the

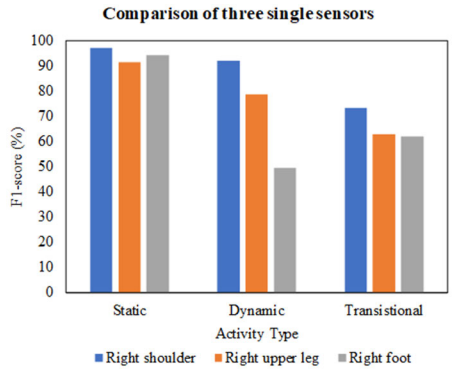


**FIGURE 7.** F1-score of the three single sensors related to three types of activity.

rate of recognition is the variance of the other two kinds of activity classification, especially dynamic activity classification. Based on Figure 7, the signal from the right foot cannot effectively discriminate between dynamic activities. In its related confusion matrix, the trained classifier has a worse capacity to classify the activities ''going upstairs'' and ''going downstairs.'' The same situation also emerges for the right upper leg sensor. For transitional activity recognition, none of the three sensors has relatively good performance in classifying a reversible transitional activity. However, increasing the number of sensors can improve the situation.

### 2) MORE THAN ONE SENSOR USED EVALUATED WITH OPTIMAL LAYOUT

Figure 8 shows the confusion matrix of two-, three- and four-sensor optimal combinations found by the MSMS-DPSO algorithm. The F1 scores for respective types of activity for different numbers of sensors used is also presented in Figure 8. With many more sensors used, the most obvious improvement related to the prediction of results is the classification of transitional activities. The F1 score of this type of activity increases from 73.31% (one sensor used) to 88.49% (four sensors used). For dynamic activities, the F1 score of only one sensor used on the right shoulder is 92.04%, while a four-sensor combination raises the score to 97.65%. For these two kinds of activity, increasing the number of sensors contributes to a better performance for the SVM classifier. However, a continual increase in the number of sensors does not generate a significant improvement. For static activities, the right shoulder sensor used alone can offer an adequate classification accuracy of 96.98%. For four sensors used, the highest accuracy achieved is 98.79%. So, compared with identifying the two other types of activities, varying the number of sensors does not significantly improve the classifier's performance for static activities.

These results provide the basic information for human ADL recognition using an accelerometer. Among 17 different positions on the human body, using accelerometers on the upper body with the SVM classifier provides an acceptable result. For recognizing static activity, any location for accelerometers can produce an adequate classification result. However, signals from lower body sensors generally have less ability to identify the actions of going upstairs and downstairs as well as transitional activities. If a better result is required, especially for the recognition of transitional activities, increasing the number of sensors can be a favorable solution.

### 3) SENSOR LAYOUT BASED ON USER PREFERENCE

As mentioned before, one important factor of applying the HAR system to individuals is where the wearable sensor should be worn. The selection of sensor position not only determines the prediction performance of the system but also depends on the user's actual physical situation. For practical application, we proposed that considering the user's demand and preference for sensor positions is significant. Thus, we examined several sensor combinations based on the specific positions on the body that fit the user's demand and conditions.

To present the usage of our method to satisfy different user conditions, we investigated user preferences for the placement of wearable devices using an online questionnaire. There were 100 respondents (50 male and 50 female) aged between 20 and 60 involved in the online survey. The involved participants number is common from the related community [2], [50]. The results are shown in Figure. 10.

Although different people have different demands for wearable sensor position, more than half of people prefer to wear the sensor on the wrist. Also, some would like to keep the device on the head or glasses. Via the proposed MSMS-DPSO algorithm, we can examine several combinations with specific user-preferred positions as the fixed positions. The relevant results are shown in Table 7.

## VI. DISCUSSION

According to the results, sensors on the upper body show better performance in detecting a series of human ADL, especially the *waist*, *chest*, *head*, and *shoulder*. As Figure 10 shows, the *waist* is given the highest ranking, which is consistent with the work of [20]. However, in our work, we contributed to the generation of more sensor layouts when the designated sensor placement is ineffective due to the physical condition or preference of the user.

When more sensors are adopted to increase the accuracy of the results, the best results come from combining the *waist* sensor, *chest* sensor, *head* sensor, *shoulder* sensor, and *upper arm* sensor. Nevertheless, we found no notable improvement in accuracy when the number of sensors used exceeded two. This is similar to Cleland's results [7], but their work did not consider transitional activity. Additionally, with increasing number of sensors, the most significant improvement is seen for dynamic and transitional activity, especially the latter. But for static activity, one sensor can provide acceptable classification results. Compared with the related literature, our work is relatively more comprehensive, using 17 accelerometers

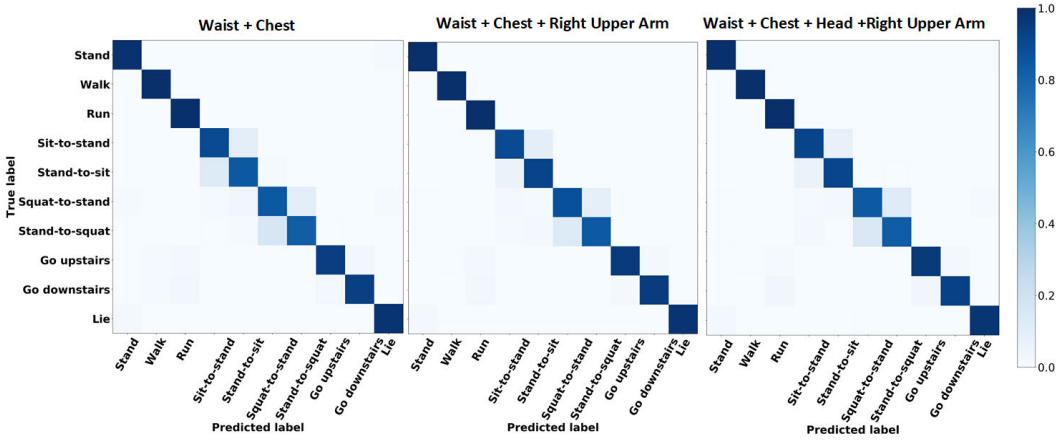


**FIGURE 8.** The confusion matrix of optimal two-sensor, three-sensor, and four-sensor combinations.

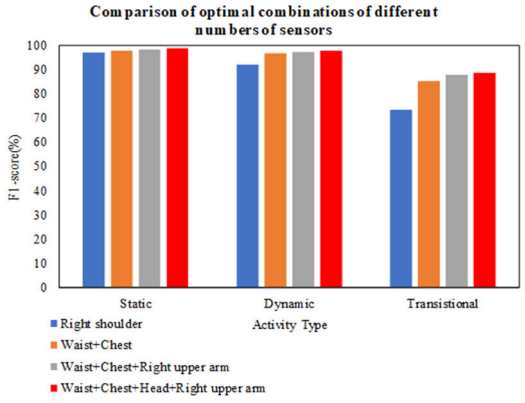


**FIGURE 9.** F1-score of optimal two-, three- and four-sensor combination related to three types of activity.

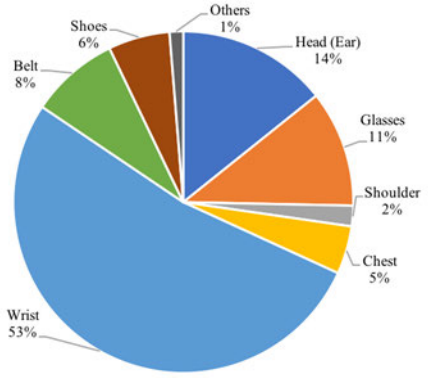


**FIGURE 10.** The investigation of user preference for wearable device.

placed on different locations of the human body to investigate the effect of various numbers and positions of sensors on classification performance.

As sensor position has been given close attention, many researchers have investigated the influence of sensor position on the performance of an HAR system from various vantage points, such as exploring the best position [11], [33], validating different classifiers [20], [37], testing sensor numbers [36], and examining the position-specific classifier [20], [21]. However, based on not only previous investigation results but also the findings of this paper, the optimal sensor placement depends on the specific HAR system as well as recognized activities. The discussed optimal sensor placement is supposed to be under certain conditions. In contrast to concentrating on the study of a recognition algorithm, focusing on sensor position ultimately aims to leave the sensor selection in the hands of the end user and maintain the user-to-sensor interaction in such wearable HAR systems. Thus, the optimization perspective proposed in this paper not only aims to investigate which part of the human body is most suitable for accelerometer placement but also intends to combine the user's preferences and demands to produce a flexible sensor layout scheme. Not limited to the conclusions obtained from previous works, this paper expands the examined positions of wearable sensors based on the rigid body model and the symmetry of the human body. The optimization scheme developed has the general ability to fit different HAR systems and offer different optimal solutions.

However, there are still some limitations and shortages in this research. Because the paper concentrated more on the optimization scheme, only some simple activities were selected. While, to better sever more people, more types of activities could be considered, such as context-aware activities in daily life. Furthermore, although we proposed the searching algorithm based on DPSO for addressing relevant sensor selection issues, the slow operating speed only allows this algorithm to be applied in an offline scenario. Using a rapid optimization algorithm is more likely to allow the related sensor selection system to be utilized in online optimization scenarios, allowing for more applications. Moreover, the survey of user's preference can be recognized as only a preliminary result. We considered the other works and merely conducted a small range investigation

**TABLE 7.** Result with specific positions.

| Specific Position | Optimal combination | | F1-Score | | |
|---|---|---|---|---|---|
| | | | Static | Dynamic | Transitional |
| Waist | 2 | + Chest | 97.09% | 96.46% | 84.86% |
| | 3 | + Chest + Right Upper arm | 98.07% | 97.12% | 86.26% |
| | 4 | +Head + Chest + Right Upper Arm | 98.52% | 97.55% | 88.11% |
| Chest | 2 | +Waist | 97.09% | 96.46% | 84.86% |
| | 3 | + Waist + Right Upper Arm | 98.07% | 97.12% | 86.26% |
| | 4 | +Head + Chest + Right Upper Arm | 98.52% | 97.55% | 88.11% |
| Head | 2 | +Waist | 97.04% | 96.09% | 82.52% |
| | 3 | + Waist + Chest | 98.30% | 97.68% | 85.93% |
| | 4 | +Head + Chest + Right Upper Arm | 98.52% | 97.55% | 88.11% |
| Shoulder (R) | 2 | +Waist | 97.58% | 95.77% | 82.83% |
| | 3 | +Waist + Head | 98.68% | 96.85% | 85.37% |
| | 4 | + Waist + Chest +Right Upper Arm | 99.07% | 97.05% | 86.56% |
| Upper Arm (R) | 2 | + Chest | 98.02% | 95.05% | 79.21% |
| | 3 | +Waist + Chest | 98.07% | 97.12% | 86.26% |
| | 4 | +Head + Chest + Right Upper Arm | 98.52% | 97.55% | 88.11% |
| Forearm (R) | 2 | +Right Shoulder | 96.16% | 93.67% | 77.37% |
| | 3 | +Waist +Head | 97.91% | 95.09% | 83.48% |
| | 4 | +Head + Right Shoulder + Left Upper Arm | 98.03% | 95.61% | 82.33% |
| Upper leg (R) | 2 | + Right Shoulder | 97.09% | 84.37% | 81.31% |
| | 3 | +Waist + Head | 98.12% | 86.99% | 86.28% |
| | 4 | +Waist +Chest + Head | 98.89% | 85.64% | 87.73% |
| Lower leg (R) | 2 | + Right Shoulder | 97.42% | 81.95% | 80.28% |
| | 3 | +Waist + Head | 97.75% | 83.54% | 86.15% |
| | 4 | +Waist +Chest + Head | 98.63% | 87.78% | 86.62% |
| Foot (R) | 2 | + Right Shoulder | 99.28% | 60.28% | 78.43% |
| | 3 | + Right Shoulder | 98.96% | 64.46% | 83.69% |
| | 4 | +Waist + Head | 99.57% | 68.10% | 86.23% |

(100 participants) to acquire the user's preference. It is believed that the results will be more convincing with the increase of participant's diversity. While the focus of this study is related to the optimal sensor position derivation, we used the results from survey to demonstrate that the user's conditions are different and proposed method can be employed to output the optimal sensor positions according to the user's conditions.

## VII. CONCLUSION AND FUTURE WORK

This paper studied the impact of the number and placement of accelerometers on human daily activity recognition. Two methods, the greedy approach and the developed MSMS-DPSO, were proposed to investigate the issue of sensor layout

**Algorithm 1** . Implementation of MSMS-DPSO

**Input:** Swarm number: *Swarm*; Particles in each swarm: *Particle*; Dimension number $N$; Current position $x$; Local best position $Pb$; Global best position $Gb$;
**Output:** Best position $Gb$ and its fitness value

Set parameters of velocity updating formula;
**1) Initialization**
Velocity randomly assigned between $[-1,1]$
$\{x\}$ [2] ← Particle position initialization algorithm
$\{Pb\}$ and $\{Gb\}$ ← Fitness calculation
**2): Intragroup Optimization**
**while** no stop condition satisfied **do**
  **for** $i = 0$ to *Swarm* * *Particle* *$N$ **do**
    **if** $x$[k] not equal to $Gb$[k] **then**
      $v^k_{n+1}$ ←Velocity updating and set $\pm 1$ as limitation
      $x'^k_{n+1} \leftarrow x^k_{n+1}$ & $v^k_{n+1}$
      Non-repetition algorithm and position limitation;
      $\{Pb\}$ and $\{Gb\}$ ← Fitness calculation
    **end if**
  **end for**
**end while**
**3) Whole Swarm Optimization**
$\{x\} \leftarrow \{Pb\}$; $\{Pb\} \leftarrow \{Gb\}$; $Gb \leftarrow \max\{Gb\}$;
**while** no stop condition satisfied **do**
  **for** $i = 0$ to *Swarm* *$N$ **do**
    **if** $x$[k] not equal to $Gb$[k] **then**
      $v^k_{n+1}$ ← Velocity updating and set $\pm 1.6$ as limitation
      $x'^k_{n+1} \leftarrow x^k_{n+1}$ & $v^k_{n+1}$
      Non-repetition algorithm and position limitation;
    **end if**
    **if** position has been altered **then**
      $\{Pb\}$ and $\{Gb\}$ ← Fitness calculation
    **end if**
  **end for**
**end while**

on the body. The results from these methods reveal that with an increase in the number of sensors used, the average prediction accuracy can be effectively improved, particularly when the number increases from one to two. A subtle improvement in accuracy is seen when the sensor number is higher than four. The proposed MSMS-DPSO optimization scheme can be used to produce the best sensor layout based on specific positions as a premise for accommodating different user demands. The designed system aims to maintain the user's selection regarding sensor placement and keeps the interface between the HAR system and user to generate a more individualized pervasive sensing system.

Based on the results, different body segments generate different levels of accuracy in HAR response, and upper and lower body sensors show significant variance in dynamic and transitional activity recognition. With more sensors used, classification performance in terms of transitional activity effectively improves. If the recognized activities basically consist of static and dynamic activities, two sensors can produce acceptable results. A sensor placed on the upper body (waist, chest, head, shoulder, upper arm, in order of relative performance) maintains an increasing prediction ability in various types of activity recognition.

The optimization scheme helps the HAR obtain a more flexible sensor position interface to realize the personalization of the user, such as some training cases for patients [51]. To better push forward the method result of this study, the next step is likely to keep on building an lightweight system fusing the optimization scheme to better support the HAR system design, and also consider more factor in the design period besides the user's preference, like the sensor weight and cost, which is going to seek a multi-dimensional optimization scheme to benefit the decision making in the wearable HAR systems [52].

## APPENDIXS

See Algorithm 1.

## REFERENCES

[1] L. Xue, S. Xiandong, N. Lanshun, L. Jiazhen, D. Renjie, Z. Dechen, and C. Dianhui, "Understanding and improving deep neural network for activity recognition," 2018, *arXiv:1805.07020*.
[2] A. Danilova, A. Naiakshina, and M. Smith, "One size does not fit all: A grounded theory and online survey study of developer preferences for security warning types," in *Proc. ACM/IEEE 42nd Int. Conf. Softw. Eng. (ICSE)*, Jun. 2020, pp. 136–148.
[3] J. Kulchyk and A. Etemad, "Activity recognition with wearable accelerometers using deep convolutional neural network and the effect of sensor placement," in *Proc. IEEE SENSORS*, Oct. 2019, pp. 1–4.
[4] K.-H. Chen, P.-C. Chen, K.-C. Liu, and C.-T. Chan, "Wearable sensor-based rehabilitation exercise assessment for knee osteoarthritis," *Sensors*, vol. 15, no. 2, pp. 4193–4211, Feb. 2015.
[5] T. Rault, A. Bouabdallah, Y. Challal, and F. Marin, "A survey of energy-efficient context recognition systems using wearable sensors for healthcare applications," *Pervasive Mobile Comput.*, vol. 37, pp. 23–44, Jun. 2017.
[6] W. H. Wu, A. A. T. Bui, M. A. Batalin, D. Liu, and W. J. Kaiser, "Incremental diagnosis method for intelligent wearable sensor systems," *IEEE Trans. Inf. Technol. Biomed.*, vol. 11, no. 5, pp. 553–562, Sep. 2007.
[7] L. Wang, T. Gu, X. Tao, and J. Lu, "A hierarchical approach to real-time activity recognition in body sensor networks," *Pervasive Mobile Comput.*, vol. 8, no. 1, pp. 115–130, Feb. 2012.
[8] S. J. Preece, J. Y. Goulermas, L. P. J. Kenney, D. Howard, K. Meijer, and R. Crompton, "Activity identification using body-mounted sensors—A review of classification techniques," *Physiol. Meas.*, vol. 30, no. 4, pp. R1–R33, Apr. 2009.
[9] C. Zhu and W. Sheng, "Motion- and location-based online human daily activity recognition," *Pervasive Mobile Comput.*, vol. 7, pp. 256–269, Apr. 2011.
[10] S. Ji, W. Xu, M. Yang, and K. Yu, "3D convolutional neural networks for human action recognition," *IEEE Trans. Pattern Anal. Mach. Intell.*, vol. 35, no. 1, pp. 221–231, Jan. 2013.
[11] L. Atallah, B. Lo, R. King, and G.-Z. Yang, "Sensor positioning for activity recognition using wearable accelerometers," *IEEE Trans. Biomed. Circuits Syst.*, vol. 5, no. 4, pp. 320–329, Aug. 2011.
[12] G. Wang, Q. Li, L. Wang, W. Wang, M. Wu, and T. Liu, "Impact of sliding window length in indoor human motion modes and pose pattern recognition based on smartphone sensors," *Sensors*, vol. 18, no. 6, p. 1965, Jun. 2018.
[13] Y. Chen and C. Shen, "Performance analysis of smartphone-sensor behavior for human activity recognition," *IEEE Access*, vol. 5, pp. 3095–3110, 2017.
[14] W. Jiang and Z. Yin, "Human activity recognition using wearable sensors by deep convolutional neural networks," in *Proc. 23rd ACM Int. Conf. Multimedia*, Oct. 2015, pp. 1307–1310.
[15] C. A. Ronao and S.-B. Cho, "Human activity recognition with smartphone sensors using deep learning neural networks," *Expert Syst. Appl.*, vol. 59, pp. 235–244, Oct. 2016.
[16] J. Yang, M. N. Nguyen, P. P. San, X. L. Li, and S. Krishnaswamy, "Deep convolutional neural networks on multichannel time series for human activity recognition," in *Proc. 24th Int. Joint Conf. Artif. Intell.*, 2015, pp. 1–7.
[17] A. G. Bonomi, A. H. C. Goris, B. Yin, and K. R. Westerterp, "Detection of type, duration, and intensity of physical activity using an accelerometer," *Med. Sci. Sports Exerc.*, vol. 41, no. 9, pp. 1770–1777, Sep. 2009.
[18] J. Liu, L. Zhong, J. Wickramasuriya, and V. Vasudevan, "UWave: Accelerometer-based personalized gesture recognition and its applications," *Pervasive Mobile Comput.*, vol. 5, no. 6, pp. 657–675, Dec. 2009.
[19] N. C. Krishnan and D. J. Cook, "Activity recognition on streaming sensor data," *Pervasive Mobile Comput.*, vol. 10, pp. 138–154, Feb. 2014.
[20] T. Sztyler and H. Stuckenschmidt, "On-body localization of wearable devices: An investigation of position-aware activity recognition," in *Proc. IEEE Int. Conf. Pervasive Comput. Commun. (PerCom)*, Mar. 2016, pp. 1–9.
[21] A. Mannini, A. M. Sabatini, and S. S. Intille, "Accelerometry-based recognition of the placement sites of a wearable sensor," *Pervasive Mobile Comput.*, vol. 21, pp. 62–74, Aug. 2015.
[22] B.-Y. Su, J. Wang, S.-Q. Liu, M. Sheng, J. Jiang, and K. Xiang, "A CNN-based method for intent recognition using inertial measurement units and intelligent lower limb prosthesis," *IEEE Trans. Neural Syst. Rehabil. Eng.*, vol. 27, no. 5, pp. 1032–1042, May 2019.
[23] Y. Chang, A. Mathur, A. Isopoussu, J. Song, and F. Kawsar, "A systematic study of unsupervised domain adaptation for robust human-activity recognition," *Proc. ACM Interact., Mobile, Wearable Ubiquitous Technol.*, vol. 4, no. 1, pp. 1–30, Mar. 2020.
[24] R. Gravina, P. Alinia, H. Ghasemzadeh, and G. Fortino, "Multi-sensor fusion in body sensor networks: State-of-the-art and research challenges," *Inf. Fusion*, vol. 35, pp. 68–80, May 2017.
[25] M. Panwar, D. Biswas, H. Bajaj, M. Jöbges, R. Turk, K. Maharatna, and A. Acharyya, "Rehab-Net: Deep learning framework for arm movement classification using wearable sensors for stroke rehabilitation," *IEEE Trans. Biomed. Eng.*, vol. 66, no. 11, pp. 3026–3037, Nov. 2019.
[26] S. Patel, H. Park, P. Bonato, L. Chan, and M. Rodgers, "A review of wearable sensors and systems with application in rehabilitation," *J. NeuroEng. Rehabil.*, vol. 9, no. 1, pp. 1–17, Dec. 2012.
[27] D. Ravi, C. Wong, B. Lo, and G.-Z. Yang, "A deep learning approach to on-node sensor data analytics for mobile or wearable devices," *IEEE J. Biomed. Health Informat.*, vol. 21, no. 1, pp. 56–64, Jan. 2017.
[28] X. Su, H. Tong, and P. Ji, "Accelerometer-based activity recognition on smartphone," in *Proc. 23rd ACM Int. Conf. Conf. Inf. Knowl. Manage.*, Nov. 2014, pp. 2021–2023.
[29] S.-M. Lee, S. Min Yoon, and H. Cho, "Human activity recognition from accelerometer data using convolutional neural network," in *Proc. IEEE Int. Conf. Big Data Smart Comput. (BigComp)*, Feb. 2017, pp. 131–134.
[30] P. Blanloeuil, N. A. E. Nurhazli, and M. Veidt, "Particle swarm optimization for optimal sensor placement in ultrasonic SHM systems," *Proc. SPIE*, vol. 9804, Apr. 2016, p. 98040.
[31] E. B. Flynn and M. D. Todd, "A Bayesian approach to optimal sensor placement for structural health monitoring with application to active sensing," *Mech. Syst. Signal Process.*, vol. 24, no. 4, pp. 891–903, May 2010.
[32] V. Mallardo, M. H. Aliabadi, and Z. S. Khodaei, "Optimal sensor positioning for impact localization in smart composite panels," *J. Intell. Mater. Syst. Struct.*, vol. 24, no. 5, pp. 559–573, Mar. 2013.
[33] K. Kunze and P. Lukowicz, "Dealing with sensor displacement in motion-based onbody activity recognition systems," in *Proc. 10th Int. Conf. Ubiquitous Comput.*, 2008, pp. 20–29.
[34] H. Gjoreski and M. Gams, "Activity/posture recognition using wearable sensors placed on different body locations," in *Proc. Signal Image Process. Appl.*, Crete, Greece, vol. 2224, 2011, p. 716724.
[35] D. O. Olguın and A. S. Pentland, "Human activity recognition: Accuracy across common locations for wearable sensors," in *Proc. 10th IEEE Int. Symp. Wearable Comput.* Montreux, Switzerland: Citeseer, Oct. 2006, pp. 11–14.
[36] I. Cleland, B. Kikhia, C. Nugent, A. Boytsov, J. Hallberg, K. Synnes, S. McClean, and D. Finlay, "Optimal placement of accelerometers for the detection of everyday activities," *Sensors*, vol. 13, no. 7, pp. 9183–9200, Jul. 2013.
[37] O. C. Kurban and T. Yıldırım, "Daily motion recognition system by a triaxial accelerometer usable in different positions," *IEEE Sensors J.*, vol. 19, no. 17, pp. 7543–7552, Sep. 2019.
[38] K. J. Kubota, J. A. Chen, and M. A. Little, "Machine learning for large-scale wearable sensor data in Parkinson's disease: Concepts, promises, pitfalls, and futures," *Movement Disorders*, vol. 31, no. 9, pp. 1314–1326, Sep. 2016.

[39] M. Cornacchia, K. Ozcan, Y. Zheng, and S. Velipasalar, "A survey on activity detection and classification using wearable sensors," *IEEE Sensors J.*, vol. 17, no. 2, pp. 386–403, Jan. 2017.
[40] M. Zubair, K. Song, and C. Yoon, "Human activity recognition using wearable accelerometer sensors," in *Proc. IEEE Int. Conf. Consum. Electron.-Asia (ICCE-Asia)*, Oct. 2016, pp. 1–5.
[41] J. Wu and R. Jafari, "Orientation independent activity/gesture recognition using wearable motion sensors," *IEEE Internet Things J.*, vol. 6, no. 2, pp. 1427–1437, Apr. 2019.
[42] F. Li, K. Shirahama, M. Nisar, L. Köping, and M. Grzegorzek, "Comparison of feature learning methods for human activity recognition using wearable sensors," *Sensors*, vol. 18, no. 3, p. 679, Feb. 2018.
[43] O. Chapelle, V. Vapnik, O. Bousquet, and S. Mukherjee, "Choosing multiple parameters for support vector machines," *Mach. Learn.*, vol. 46, pp. 131–159, Jan. 2002.
[44] S. J. Preece, J. Y. Goulermas, L. P. Kenney, and D. Howard, "A comparison of feature extraction methods for the classification of dynamic activities from accelerometer data," *IEEE Trans. Biomed. Eng.*, vol. 56, no. 3, pp. 871–879, Mar. 2009.
[45] M. Rosendo and A. Pozo, "Applying a discrete particle swarm optimization algorithm to combinatorial problems," in *Proc. 11th Brazilian Symp. Neural Netw.*, Oct. 2010, pp. 235–240.
[46] Y. D. Valle, G. K. Venayagamoorthy, S. Mohagheghi, J.-C. Hernandez, and R. G. Harley, "Particle swarm optimization: Basic concepts, variants and applications in power systems," *IEEE Trans. Evol. Comput.*, vol. 12, no. 2, pp. 171–195, Apr. 2008.
[47] J. Huang, M. Gong, and L. Ma, "A global network alignment method using discrete particle swarm optimization," *IEEE/ACM Trans. Comput. Biol. Bioinf.*, vol. 15, no. 3, pp. 705–718, May 2018.
[48] J. Kennedy and R. C. Eberhart, "A discrete binary version of the particle swarm algorithm," in *Proc. IEEE Int. Conf. Syst., Man, Cybern. Comput. Cybern. Simulation*, Oct. 1997, pp. 4104–4108.
[49] T. Tianhan, W. Kun, W. Qishuang, F. Bo, W. Gang, and L. Yongsheng, "UAV cooperative attack and route planning based on DPSO algorithm," *J. Phys., Conf. Ser.*, vol. 1345, no. 4, Nov. 2019, Art. no. 042040.
[50] N. Herbig, P. Schuck, and A. Krüger, "User acceptance of cognition-aware e-learning: An online survey," in *Proc. 18th Int. Conf. Mobile Ubiquitous Multimedia*, Nov. 2019, pp. 1–6.
[51] M. Toriumi, Y. Sugiura, and K. Fujita, "An application for wrist rehabilitation using smartphones," in *Proc. 21st Int. Conf. Hum.-Comput. Interact. Mobile Devices Services*, Oct. 2019, p. 65.
[52] Z. Ali, T. Mahmood, and M. S. Yang, "Complex T-spherical fuzzy aggregation operators with application to multi-attribute decision making," *Symmetry*, vol. 12, no. 8, p. 1311, 2020.

**CHENGSHUO XIA** received the B.Sc. degree in automation from the Xi'an University of Technology, in 2016, the M.Sc. degree in electronic and electrical engineering from Loughborough University, in 2018, and the master's degree in control theory and control engineering from Xidian University, in 2019. He is currently pursuing the Ph.D. degree with Keio University, Japan. His research interests include wearable computing, human–computer interaction, and energy harvesting.

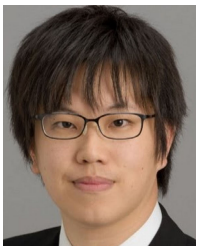

**YUTA SUGIURA** received the Ph.D. degree from the Graduate School of Media Design, Keio University, in 2013. He is currently an Associate Professor with the Department of Information and Computer Science, Keio University. Before joining the department, he worked as a Postdoctoral Researcher at the National Institute of Advanced Industrial Science and Technology, from 2015 to 2016. His research interests include user interfaces and ubiquitous computing. He served as a Program Committee Member for various international conferences, including ACM UIST, TEI, and SIGGRAPH ASIA E-Tech. He has received several awards, including the IPSJ Prize, the UIST Best Talk Award, and the Good Design Award.